MICROMIRROR BASED OPTICAL PHASED ARRAY FOR WIDE-ANGLE BEAMSTEERING

*Youmin Wang, and Ming C. Wu**
University of California, Berkeley, Berkeley, USA

ABSTRACT

Optical phased array (OPA) is a key enabling element for solid state LIDAR (light detection and ranging). In this paper, we demonstrate a novel MEMS micromirror array OPA. Vertical combdrive actuators are integrated underneath the mirrors to achieve a small pitch (2.4μm) and a large field of view (22° at 905nm wavelength and 40° at 1550nm). The OPA has 2μs response time, and 10V actuation voltage.

INTRODUCTION

Compact light-detection-and-ranging (LIDAR) devices are of intense interests for their applications in self-driving cars and autonomous vehicles [1]. Optical phased arrays (OPAs) are key enabling elements for compact solid-state LIDAR (light detection and ranging) for three-dimensional imaging without bulk mechanical moving parts [2]. In addition to beam scanning, the OPAs are capable of sophisticated beamforming such as simultaneous scanning, pointing, and tracking of multiple objects. Aside from LIDAR, OPA also has applications in 3D display, computational imaging and microscopy, digital holography, and free-space line-of-sight optical communications.

OPAs with several types of phase modulators have been reported. Liquid crystals are most commonly used for large-scale OPAs [3], but they are too slow for automotive LIDAR. Silicon photonic waveguides with phase modulators and grating couplers have been reported recently, however, they have high insertion loss and are limited to infrared wavelengths transparent to Silicon [4]. MEMS offers high speed operation and sharp phase transitions, both are attractive for scanning LIDAR. OPAs with digital micromirror arrays have been used to implement fast fiber optic switches [5], but they suffer from low diffraction efficiency in amplitude-modulated phased array. Piston mirror-based OPA with microsecond response time, low energy consumption, and high optical efficiency was recently reported, but the large mirror size (22μm) limits their scan angles to 4 degrees [6].

In this paper, we report on a novel one-dimensional (1-D) MEMS OPA with piston mirrors integrated on top of vertical combdrive actuators. This allows us to achieve a smaller pitch (2.4μm) and a large scan angle (22° at 905nm wavelength) than all previously reported MEMS OPAs. Since micromirror is a broadband reflective device, the OPA can operate at other wavelength, or multiple wavelengths simultaneously. At 1550nm, a larger scan angle of 37.7° can be realized. The vertical combdrive actuators with submicron fingers/gaps (300nm) enable us to achieve fast time response and low operation voltage. The resonance frequency is measured at 310kHz and the actuation voltage is 10V.

MEMS OPA DESIGN AND FABRICATION

The optical performance of an OPA is determined by its pitch, aperture, and the number of elements in the array. The device consists of a one-dimensional array of micromirrors. Each mirror is 2.1μm wide and 30μm long. The pitch of the OPA is designed to be 2.4μm, resulting in 87.5% fill-factor. The maximum beam steering angle without magnification optics is given by

$$\theta = \pm\sin\left(\frac{\lambda}{2\Lambda}\right) = \pm 11°$$

where $\lambda = 905\text{nm}$ is the operating wavelength, $\Lambda = 2.4\mu\text{m}$ is the element pitch of the 1-D OPA, and $\theta = 22°$ is the field of view (maximum scan angle) at 905nm. We have designed our OPA for 100m ranging distance with 256 resolvable spots.

The schematic of our OPA device is shown in Fig. 1. To achieve high fill factor while minimizing the crosstalk between adjacent mirrors, we integrate the vertical combdrive actuators directly under the mirror. Each actuator consists of two lower and one upper comb fingers. The mirrors are tethered to anchors through a pair of springs. The mirrors and the top combs are grounded while the bottom combs are individually addressed to produce the desired beam profiles.

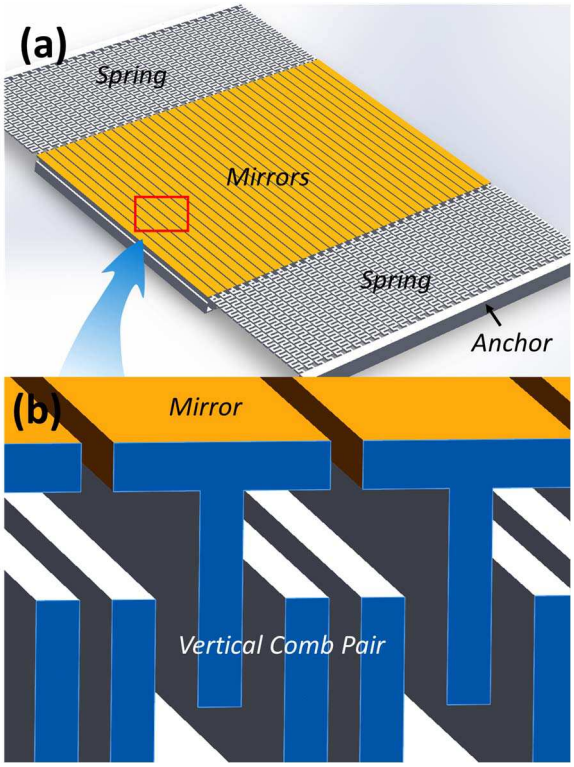

Figure 1: Schematic of the MEMS OPA device. (a) Top view of a mirror array. (b) Close-up cross-sectional view showing the mirror with the integrated vertical comb-drive structure.

The piston mirror features a resonance in the z direction at a frequency

$$f_z = \frac{1}{2\pi}\sqrt{\frac{k}{m}}$$

where k and m are the spring constant and the OPA micromirror element mass, respectively. For the double-clamped beam spring design, the spring constant can be calculated with analytical solution. Since the length of the central mirror region is rigidly enhanced by the T-shape upper comb structure, the OPA micromirror spring constant k can be simplified to be

$$\mathrm{k} = \frac{16Ewt^3}{L^3}$$

where t is the thickness of the spring layer (350nm), w is the width of the spring beam (2.1μm), and L is the total length of the spring beam (60μm). With the fixed spring constant based on the dimensions above and Young's modulus (E = 169 GPa), k = 1.248 N/m, the lightweight OPA micromirror structure has a high resonant frequency of 357.0 kHz thanks to its low mass (224 ng). The calculated resonance frequency agrees well with the finite-element-method (FEM) simulation result using ANSYS software, 318.2 kHz, as shown in Fig. 2.

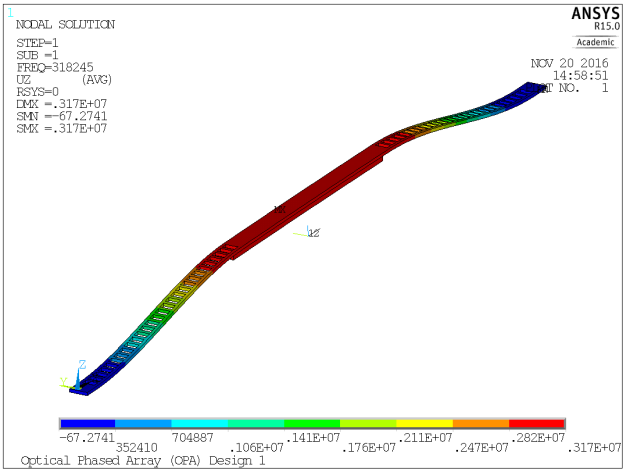

Figure 2. Modal analysis using ANSYS software showing the first resonance mode at 318.2kHz

We used a 4-mask, self-aligned surface micromachining process for the OPA fabrication, as illustrated in Fig. 3. Both the top and bottom combs are 1μm high. The widths of the comb fingers are 300nm. A deep-UV stepper (ASML 5500/300) was used to pattern the deep-submicron vertical combs. With such tightly spaced comb fingers, it is critical that the top and bottom comb fingers be self-aligned. The self-aligned process we used (step 3-6 in Fig. 3) is similar to that in Ref. [7] but with tighter control of the finger widths and spacing. To protect the integrity of the bottom comb fingers, we used a thin protective oxide sidewall when thinning the lower comb fingers (step 5-6 in Fig. 3). After releasing in HF, the device was blanket-coated with 200nm of gold to increase the reflectivity of the mirrors. The metal also provides bonding pads for electrical contacts. Polysilicon "gutters" were employed to block metals between addressing wires/bonding pads.

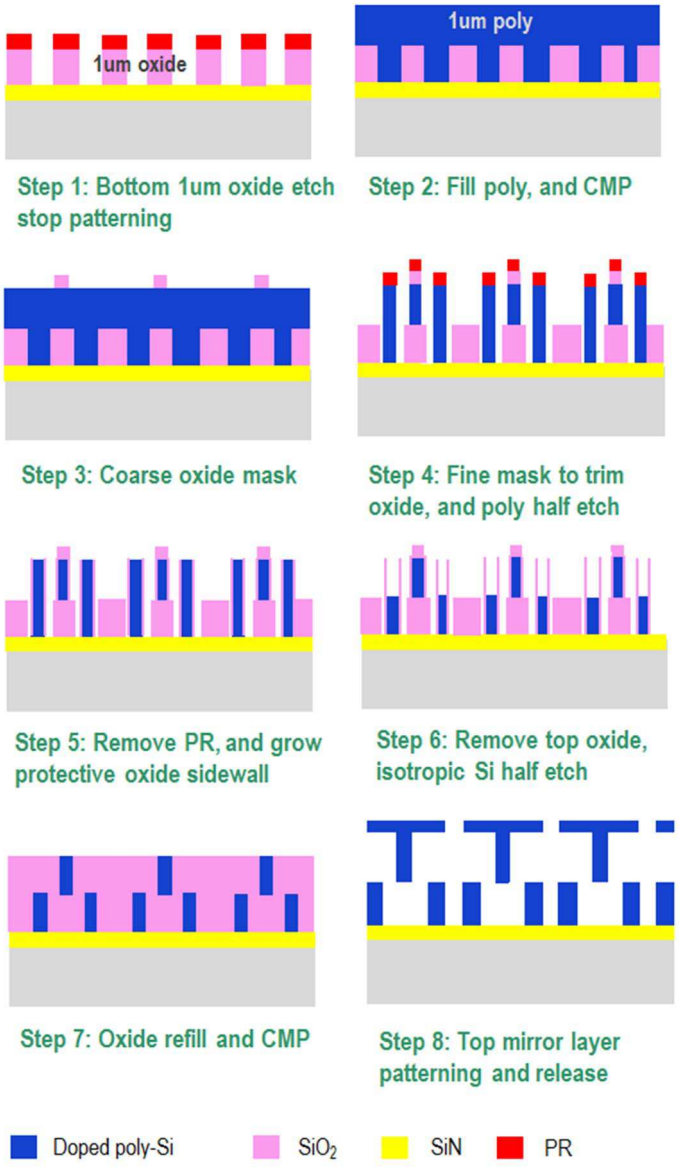

Figure 3: Fabrication process of the MEMS OPA

The scanning electron micrographs (SEMs) of fabricated 1-D OPA device is shown in Fig. 4. 256 electrical lines provide voltage biases to individual OPA micromirrors, as shown in Fig. 4(a). The electrical bias line passes the anchor of the mirrors through a tunnel, as shown in Fig. 4(b). The spring and the mirror are made of the same polysilicon layer. The spring region is etched with a perforated pattern to reduce its stiffness (Fig. 4(c)).

EXPERIMENTAL RESULTS

The released 1-D OPA device was attached and wirebonded to a printed circuit board (PCB) for electrical and optical testing. The assembled board is shown in Figure 5. The frequency response was measured with a Polytec Laser Doppler Vibrometer (LDV). The resonance frequency of the MEMS OPA is measured to be 310kHz, as shown in Figure 6(a), which agrees well with our analytical and FEM simulation results. This high resonant frequency allows for a fast response time of 2μs.

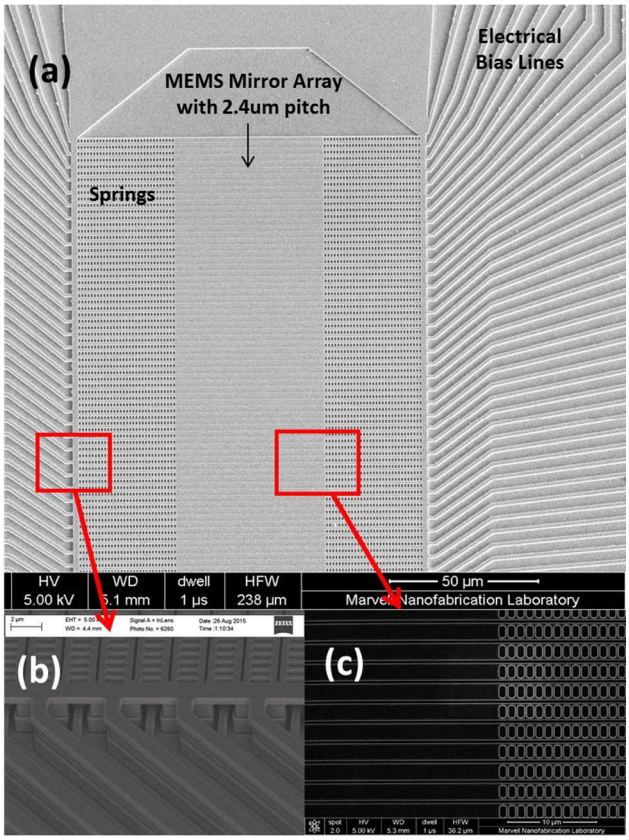

Figure 4: SEMs of the MEMS OPA. (a) Top view SEM showing arrays of micromirrors between perforated springs. (b) Close-up view of the anchor area where electrical bias lines pass through the tunnels between anchors. (c) Close-up view of the mirrors and perforated springs.

The transfer characteristics of the piston mirror is shown in Fig. 6(b). Thanks to the vertical combdrives with narrow gap spacing (300nm), 400 nm displacement is achieved at an actuation voltage of 10V. The upper comb fingers are designed to be taller than the bottom comb fingers. They provide a mechanical stop that limits the maximum displacement (to 400nm in this design) and prevents electrical short. The mirror movement is reversible after reaching the maximum displacement. The power consumption of the OPA is very low (10.7nW for each element) because of the capacitive load.

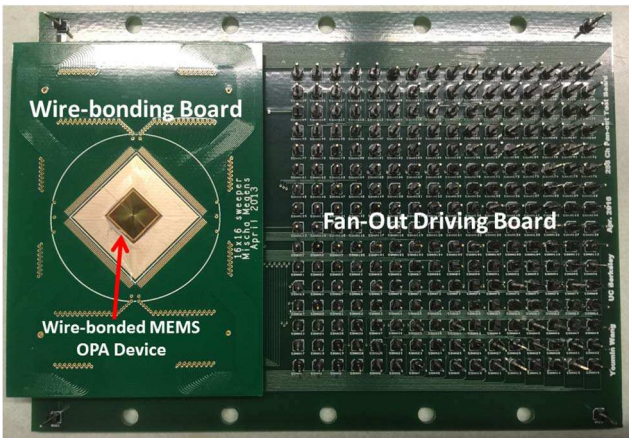

Figure 5: Photograph of the wirebonded 1-D OPA on fan-out driving printed circuit board.

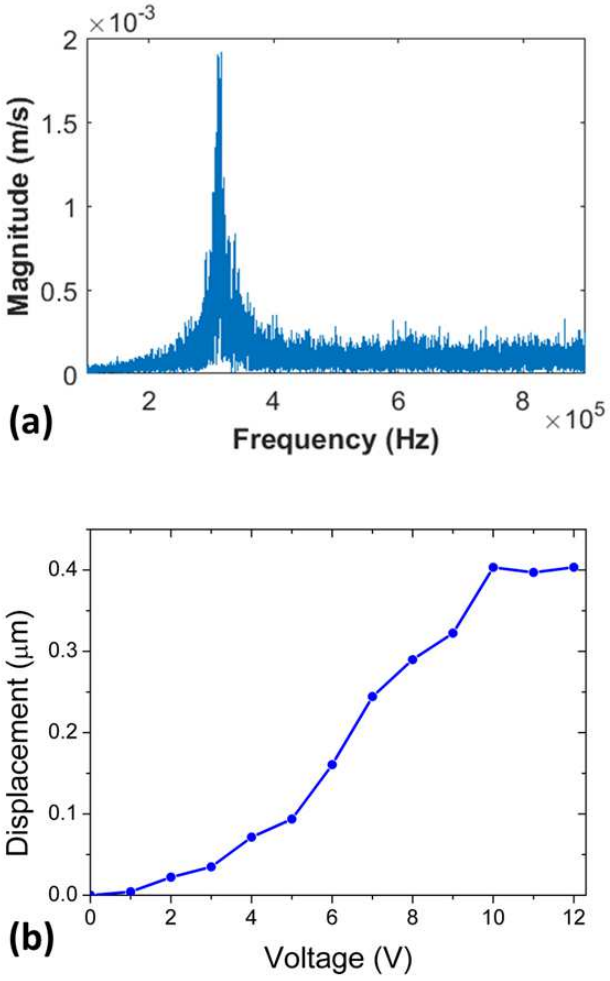

Figure 6: (a)Frequency response and (b) transfer characteristics of the piston mirror in MEMS OPA.

Surface flatness at zero bias is important for OPA as it eliminates the need for correction. The surface profile of the released OPA is measured using an Olympus confocal microscope, as shown in Fig. 7. Excluding the edge detection noise, the height difference among mirrors is < 20nm.

Due to the fine pitch and high fill factor, the micromirrors are susceptible to electrical and mechanical crosstalk, which complicates the driving algorithm and beamsteering accuracy. In our OPA, all mirrors are electrically connected to a common ground, eliminating electrostatic forces between adjacent mirrors. The mirrors are individually addressed through the fixed lower comb fingers. The electric field is well confined between the comb fingers underneath the mirror, therefore the electrostatic crosstalk between adjacent mirrors are minimized. However mechanical crosstalk could still be present through air coupling. The measured crosstalk between adjacent mirrors is about 10% when actuated at 200kHz (off resonance), as shown in Fig. 8. The displacements of adjacent mirrors are nearly 180° out of phase, suggesting the crosstalk is caused by squeezed air pressure.

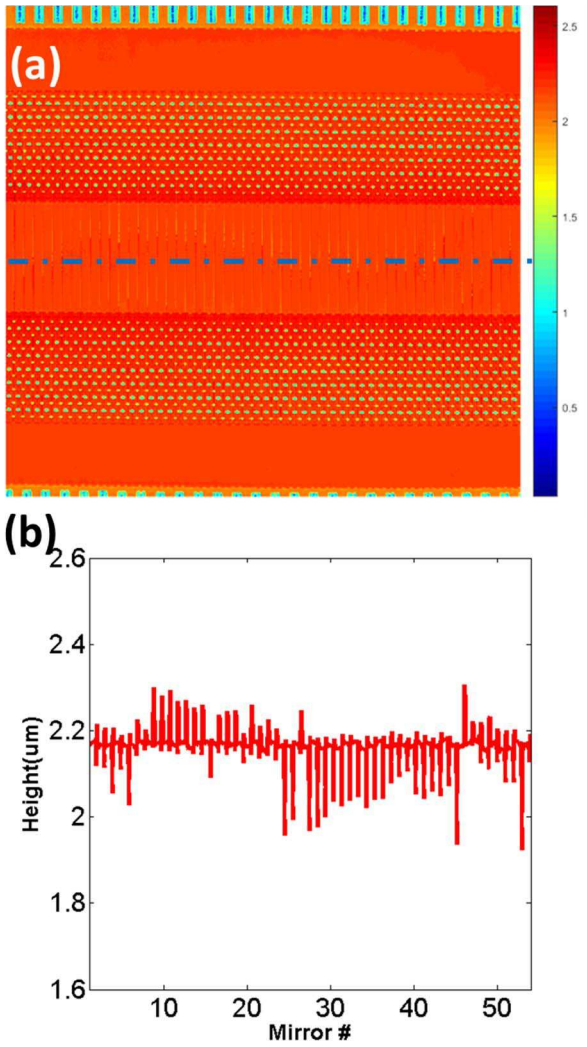

Figure 7: OPA surface profile. (a) OPA top-view surface height measurement under 3D microscope. (b) The height plot alone the blue dashed line in (a), showing uniformity within the MEMS micromirror array is <20nm.

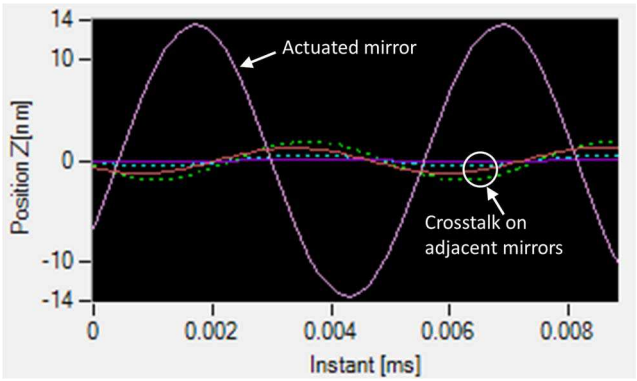

Figure 8: Displacement of actuated mirror under 200kHz actuation signal in the OPA v.s. crosstalk displacement on adjacent mirrors.

SUMMARY

We have designed and experimentally demonstrated a one-dimensional MEMS optical phased array with a fine pitch of 2.4μm. High fill factor (87.5%) and low crosstalk between adjacent mirrors are achieved with hidden vertical combdrive actuators underneath the mirrors. The mirror displacement (400nm at 10V) is sufficient for beamforming at 905nm wavelength. The 256-element array is designed for 22° field-of-view at 905nm. Low power consumption (10.7nW) is required because of capacitive load. The flatness across the mirror array at zero bias is less than 20nm. The fast response time (2μs) is compatible with automotive LIDAR requirements.

ACKNOWLEDGEMENTS

We thank Dr. Rick Oden of Texas Instruments and Dr. Niels Quack at EPFL, Switzerland, for helpful discussions. We thank Dr. Micha Megans from Phillips and Nicolas Triesault for assistance in electronics and software development. This project is funded in part by Texas Instruments (TI), Berkeley Sensors and Actuator Center (BSAC), and the NSF PFI: AIR program.

REFERENCES

[1] Levinson, Jesse, et al. "Towards fully autonomous driving: Systems and algorithms." Intelligent Vehicles Symposium (IV), 2011 IEEE. IEEE, 2011.

[2] Wang, Bin, et al. "Stressed liquid-crystal optical phased array for fast tip-tilt wavefront correction." Applied optics 44.36 (2005): 7754-7759.

[3] McManamon, Paul F., et al. "Optical phased array technology." Proceedings of the IEEE 84.2 (1996): 268-298.

[4] Hutchison, David N., et al. "High-resolution aliasing-free optical beam steering." Optica 3.8 (2016): 887-890.

[5] Lynn, Brittany, et al. "Design and Preliminary Implementation of an N × N Diffractive All-Optical Fiber Optic Switch." Journal of lightwave Technology 31.24 (2013): 4016-4021.

[6] Yoo, Byung-Wook, et al. "Optical phased array using high contrast gratings for two dimensional beamforming and beamsteering." Optics express 21.10 (2013): 12238-12248.

[7] Krishnamoorthy, Uma, et al. "Self-aligned vertical electrostatic combdrives for micromirror actuation." Microelectromechanical Systems, Journal of 12.4 (2003): 458-464.

CONTACT

*M. C. Wu, tel: +1- 510-643-0808; Email: wu@eecs.berkeley.edu